EXPERIMENTAL STUDY OF THE HADRONIC PHOTON STRUCTURE FUNCTION

The CELLO Collaboration

H.-J. BEHREND, H. FENNER, U. GÜMPEL, M.-J. SCHACHTER [1],
V. SCHRÖDER, H. SINDT
Deutsches Elektronen-Synchrotron, DESY, Hamburg, Germany

G. D'AGOSTINI, W.-D. APEL, S. BANERJEE [2], J. BODENKAMP, J. ENGLER,
G. FLÜGGE, D.C. FRIES, W. FUES, K. GAMERDINGER, G. HOPP, H. KÜSTER,
H. MÜLLER, H. RANDOLL, G. SCHMIDT, H. SCHNEIDER
Kernforschungszentrum Karlsruhe and Universität Karlsruhe, Germany

W. de BOER, G. BUSCHHORN, G. GRINDHAMMER, P. GROSSE-WIESMANN,
B. GUNDERSON, C. KIESLING, R. KOTTHAUS, U. KRUSE [3], H. LIERL,
D. LÜERS, H. OBERLACK, P. SCHACHT
Max-Planck-Institut für Physik und Astrophysik, Munich, Germany

G. CARNESECCHI [4], P. COLAS, A. CORDIER, M. DAVIER, D. FOURNIER,
J.-F. GRIVAZ, J. HAÏSSINSKI, V. JOURNÉ, F. LAPLANCHE,
F. Le DIBERDER, U. MALLIK, J.-J. VEILLET
Laboratoire de l'Accélérateur Linéaire, Orsay, France

J.H. FIELD [5], R. GEORGE, M. GOLDBERG, B. GROSSETÊTE, O. HAMON,
F. KAPUSTA, F. KOVACS, G. LONDON, L. POGGIOLI, M. RIVOAL
Laboratoire de Physique Nucléaire et des Hautes Energies, Université de Paris, France

and

R. ALEKSAN, J. BOUCHEZ, G. COZZIKA, Y. DUCROS, A. GAIDOT,
Y. LAVAGNE, J. PAMELA, J.-P. PANSART, F. PIERRE
Centre d'Etudes Nucléaires, Saclay, France

We have measured at PETRA the process $e\gamma \rightarrow e + \text{hadrons}$ at an average Q^2 value of 9 GeV^2/c^2. The total number of observed events attributed to this process is 215. Our data are compared to calculations based on the estimation of the photon structure function F_2 in the quark parton model and in QCD.

---

1. Introduction

Deep inelastic electron scattering on a photon target is considered as a good place to test the predictions of quantum chromodynamics (QCD) [1]. The photon structure functions, at high Q^2, are dominated by the point-like contribution, and can be completely calcu-

lated by perturbative QCD. This is in contrast with extended targets (nucleons, mesons) where only the evolution of the structure functions with Q^2 can be computed.

Some experimental results with lower statistical accuracy than presented here have been reported by the PLUTO collaboration [2] and recently by the JADE collaboration [3]. Preliminary results obtained with the present data have also been previously presented [4].

Experimentally, the study of deep inelastic scattering of electrons on photon targets

$$e + \gamma \rightarrow e + \text{hadrons} \qquad (1)$$

is achieved by measuring the "two-photon" reaction

$$e^+ + e^- \rightarrow e^+ + e^- + \text{hadrons} \qquad (2)$$

in configurations where one of the outgoing electrons is detected at a large angle. The corresponding Feynman graph and our notation of the associated kinematical variables are given in fig. 1. Using

$$x = -\tfrac{1}{2}q^2(\widetilde{k}\cdot\widetilde{q}) = Q^2/(Q^2 + W^2)$$

$$y = (\widetilde{k}\cdot\widetilde{q})/(\widetilde{k}\cdot\widetilde{p}) = 1 - (E'/E)\cos^2\tfrac{1}{2}\theta ,$$

the differential cross section of reaction (1) can be written, for a real photon target, as

$$d\sigma/dx\, dy = (8\pi\alpha^2/Q^4)\, EE_\gamma[1 + (1-y)^2]$$

$$\times \{F_2 + [\epsilon(y) - 1]F_L\} . \qquad (3)$$

For our experimental conditions, where y and therefore $[\epsilon(y) - 1] \simeq -y^2/2$ are small, this simplifies (provided F_2 is not too small compared to F_L) into
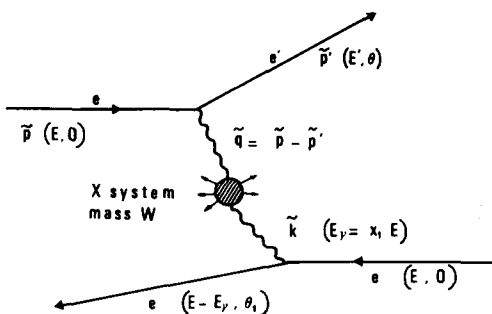
$$d\sigma/dx\, dQ^2 = (4\pi\alpha^2/Q^4)(1-y)F_2(x, Q^2)/x . \qquad (4)$$

This relation shows that the measured cross section is essentially proportional to F_2, but with a weighting factor which favours the low x region where the non-point-like VDM [5] contribution to F_2 is important.

When the electron scattered at large angle is the only one which is detected, the cross section of reaction (2) is obtained, to a good approximation [6], by a convolution of the cross section of reaction (1) with a quasi-real photon flux factor. This flux should take into account the fact that we "antitag" the second electron, i.e. that it has to be emitted at an angle with the beam smaller than θ_a (0.13 rad). Since this angle is not very small, the structure function F_2 has to incorporate correction terms depending on the squared mass $(-t)$ of the target photon. This fact has been verified in the case of lepton production in deep inelastic $e-\gamma$ scattering (see preceding letter [7]) by comparing the structure function formalism to the exact QED calculations.

2. Data collection and event selection

The data used in this analysis have been collected in 1980 and 1981 at the e^+e^- storage ring PETRA using the CELLO detectio [8]. The luminosity used for this work is 9.5 pb^{-1} and the mean beam energy is 17 GeV. The triggering conditions and the detector performances relevant for this analysis were the same as for the lepton analysis and are described in the previous letter. The hadronic system is measured using both charged particles and photon showers as reconstructed in the barrel liquid argon calorimeter with an energy cut of 0.3 GeV. The large angle scattered electron of reaction (1) and (2) is detected at polar angles between 0.13 and 0.40 rad using the end cap liquid argon calorimeters. To be considered further in the analysis, events were required to meet the following criteria:

(i) One and only one isolated shower (with $E' > 3.6$ GeV) in the end cap modules.

(ii) At least three charged particles (not including the tagged electron) with a vertex cut along the beam $\langle |Z| \rangle < 2$ cm.

(iii) The total visible energy (charged and neutral, but not including the tagged electron) lower than 40% of the total available energy $(2E_{\text{beam}})$.

(iv) The visible transverse momentum vector of the

Fig. 1. Graph and kinematics of $e^+e^- \rightarrow e^+e^- + \text{hadrons}$.

hadronic system pointing opposite to the transverse momentum of the tagged electron within ±0.8 rad.

Cut (i) is common to both hadron and lepton analyses. It implies the rejection of events which would be double-tagged. Cut (iii) rejects a large fraction of single photon annihilation events but leaves some background in our sample. To reject most of this remaining background, as well as inelastic Compton events, a further cut $E' > 8$ GeV was applied in the subsequent analysis. This together, with the lower polar angle cut, implies the cut: $Q^2 > 2.7$ GeV$^2/c^2$. We have also required that the visible invariant mass (W_{vis}) of the hadronic system be greater than 1 GeV/c^2 to be in the deep inelastic region. After these cuts we are left with 249 events.

The main possible sources of background have been studied by Monte Carlo simulations: (i) inelastic Compton scattering [5] has been found negligible in our acceptance, (ii) deep inelastic production of τ pairs corresponds to 18 events, (iii) hadronic one photon annihilation events with one π° or an initial radiation faking a tagged electron contributes 16 events. A study of the vertex position of reconstructed events has also shown that the residual beam–gas background is negligible. The different backgrounds have been subtracted bin by bin in all distributions. After this subtraction our sample contains 215 ± 17 events.

3. Data analysis

Measuring Q^2 with the tagged electron and the hadronic system as explained before, we obtained the multplicities, W_{vis} and $x_{vis} = Q^2/(Q^2 + W_{vis}^2)$ distributions which are shown in figs. 2–4 after background subtraction. Since Monte Carlo studies show that W_{vis}/W fluctuates substantially (around an average value of 0.6) it is difficult to obtain, like in the lepton case, a reliable true x distribution, from which we could deduce F_2 and then compare to theoretical predictions. We therefore follow an alternative method: we produce a sample of Monte Carlo events, which uses a suitable expression of F_2 and F_L, take into account all the known effects of our experimental detection, and then compare the obtained distributions to the experimental data.

In this simulation $e^+e^- \rightarrow e^+e^-q\bar{q}$ events are first produced according to eq. (3) using the F_2 structure functions given below, and F_L as in the quark parton model [5].
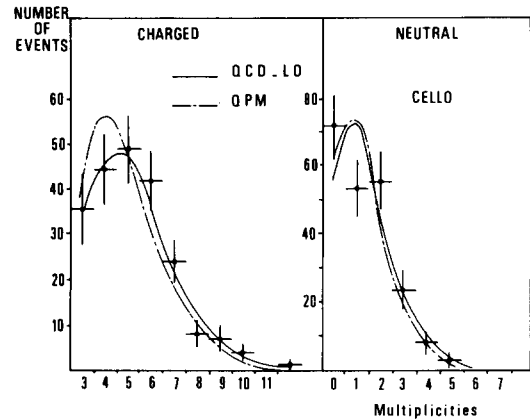

Fig. 2. Charged and neutral multiplicities. Solid dot: Data. Solid curve: QCD LO (u, d, s, c). Dash–dotted curve: QPM (u, d, s, c).

$$F_L = (4\alpha/\pi)3 \sum_i e_i^4 x^2(1 - x) . \qquad (5)$$

The target photon flux used is the same as the one given in the previous letter [7], and off-mass-shell effects are taken into account in the expression of F_2 as explained below. Radiative corrections are applied by allowing the electron, which suffers afterwards the
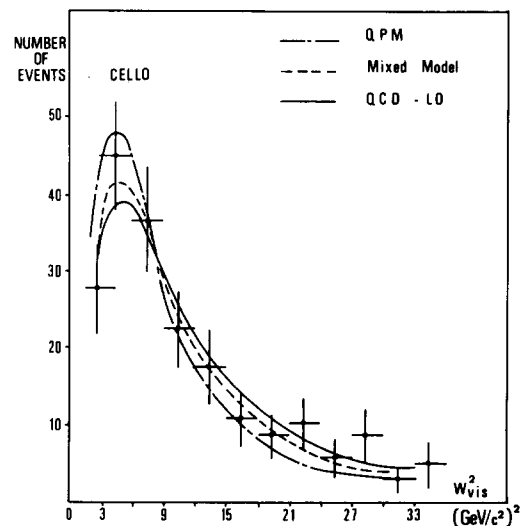

Fig. 3. W_{vis}^2 distribution. Solid dot: Data. Solid curve: QCD LO (u, d, s, c). Dashed curve: QCD LO (u, d, s) plus QPM (c). Dash–dotted curve: QPM (u, d, s, c).

Fig. 4. X_{vis} distribution. Solid dot: Data. Solid curve: QCD LO (u, d, s, c). Dashed curve: QCD LO (u, d, s) plus QPM (c). Dash—dotted curve: QPM (u, d, s, c). Dotted curve: QCD HO (u, d, s, c).
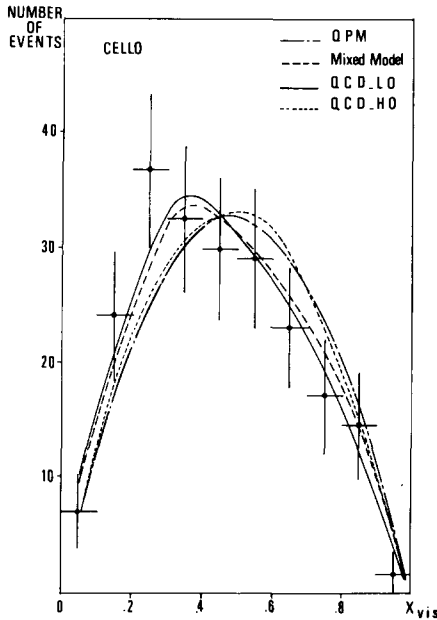
large angle scattering, to radiate (at $\theta = 0$) a photon with the usual spectrum.

In the $\gamma\gamma^*$ center of mass, the $\gamma\gamma^* \to q\bar{q}$ angular distribution is assumed to be the same as for two real photons [9]. An investigation of the deviation due to off mass-shell effects has been made; these effects are small and taken into account in our systematic errors.

In the second step the $q\bar{q}$ system is fragmented using the Lund string model [10] procedure, keeping track of the flavour (u, d, s, c) of the produced quark pair. In a third step events are passed through a simulator program which includes all known effects of the CELLO detector. Particular care is taken to account for the material (mostly aluminum) located in front of the end cap calorimeter. In the last step, events generated in this way are processed through the same reconstruction chain as the real events. The tagged electron momentum as well as the visible hadronic invariant mass and multiplicity distributions are particularly sensitive to acceptance and resolution effects. Good agreement is found at this level between data and the various models used. This can be seen in figs. 2 and 3

where we have shown the predictions of models (a) and (b) (see below) which are the extremes in our analysis.

For the dominant structure function F_2 the four following models have been used:

(a) *The quark parton model (QPM)*. We have used the complete expressions derived by Hill and Ross [11], which for light quarks and $t = 0$ reduce to

$$F_2(x, Q^2) = \frac{3\alpha}{\pi} \sum_i e_i^4 \{x[x^2 + (1-x)^2] \ln(W^2/\mu^2)$$

$$+ 8x^2(1-x) - x\}. \tag{6}$$

We have taken for the same mass μ for the three light quarks as a free parameter and we have used $m_c = 1.6$ GeV/c^2 for the charm quark.

(b) *Leading order QCD (LO)*. F_2 has been derived by many authors in the leading order of QCD [5,12–14] in the case of real photons

$$F_2(x, Q^2) = \frac{3\alpha}{\pi} \sum_i e_i^4 f(x) \ln(Q^2/\Lambda_{LO}^2). \tag{7}$$

In the present work we have used the expression of $f(x)$ of ref. [5] [$f(x) = 0.24x + 0.12$ for $0.1 < x < 0.9$], and in order to take into account the target photon mass we replaced Λ_{LO}^2 by $\Lambda_{LO}^2 + t$, in analogy with the QPM and following the work done by Uematsu and Walsh [15,16]. The charm cross section is put to zero when $W < 4$ GeV/c^2.

(c) *Mixed model*. In this model F_2 is taken according to (7) for light quarks, and according to the QPM for the charm quark.

(d) *Higher order QCD (HO)*. In next to leading order F_2 can be written [17]

$$F_2(x, Q^2) = \frac{3\alpha}{\pi} \sum_i e_i^4 \{f(x) \ln(Q^2/\Lambda_{\overline{MS}}^2)$$

$$+ g(x) \ln[\ln(Q^2/\Lambda_{\overline{MS}}^2)] + h(x)\}. \tag{8}$$

We have determined g and h from the curves obtained in the $\overline{MS}$ scheme in ref. [16], in which the effect of the target photon mass is estimated. To take most of this effect into account we have, as before, replaced $\Lambda_{\overline{MS}}^2$ by $\Lambda_{\overline{MS}}^2 + t$. Values of F_2 obtained in this work for $t = 0$ are in agreement with earlier calculations [17,18]. In particular F_2 becomes negative for $x < 0.2$. This is due to the fact that $h(x)$ is negative, and not compensated for by the other terms for low x, espe-

cially at low Q^2. In the generation of our events F_2 has been set to zero whenever formula (8) led to negative values. Due to its high mass the charm quark is treated as in (c). In each case an extra term has been added, which corresponds to the soft hadronic component of the photon. This scaling term has been calculated [5] using the vector meson dominance model. We have used

$$F_2(x) = [\alpha/(f_\rho^2/4\pi)] \tfrac{1}{4}(1 - x) ,$$

with a $\rho-\gamma$ coupling constant f_ρ such as $f_\rho^2/4\pi = 2.2$. The resulting x_{vis} distributions for models (a), (b), (c) and (d) are shown in fig. 4, and the corresponding $F_2(x)$ distributions in fig. 5. The parameters used are those corresponding to the fit in the whole x range (see below).

The sizeable differences in $F_2(x)$ between the 4 models are somewhat washed out by the $1/x$ weighting factor [see formula (4)] and the experimental errors on W, and within the present statistical accuracy, all models are compatible with the data. As indicated in

Table 1
Values of Λ (or μ) obtained in the fits to the observed number of events.

Model	all x	$x > 0.3$
(a) QPM	$0.11^{+0.07}_{-0.05}$	$0.26^{+0.11}_{-0.08}$
(b) QCD LO	$0.25^{+0.08}_{-0.06}$	$0.28^{+0.10}_{-0.08}$
(c) uds QCD LO c QPM (mixed model)	$0.08^{+0.05}_{-0.04}$	$0.13^{+0.07}_{-0.05}$
(d) uds QCD HO c QPM		$0.07^{+0.03}_{-0.02}$

ref. [16] the prediction for QCD (HO) is quite close in shape to the quark–parton model, and it should be noticed that the parton model cannot be ruled out by the present work. One can however remark that it has the tendency to slightly overestimate the high x region.

The values of Λ (or μ) for each model have been obtained by fitting the predicted number of events to the observed oves. This has been done using the whole x range, and by restricting the fit to the $x > 0.3$ region. The QCD HO value is only given for $x > 0.3$ since the low x region suffers from theoretical uncertainties. The values obtained for Λ are shown in table 1. All of them are in the range 0.05 to 0.3 GeV/c^2, i.e. compatible with what has been obtained in deep inelastic lepton–hadron scattering. They are also compatible with the result from JADE [3]. For example in the QCD (LO) model, treating the charm quark as in the parton model, we obtain [1]:

$$\Lambda = 0.13^{+0.07}_{-0.05} \text{ GeV} ,$$

where in a similar x range ($x > 0.4$) JADE obtains $\Lambda = 0.21^{+0.17}_{-0.09}$ GeV.

Systematic errors in the absolute yield of events translate into systematic errors on Λ. In the case of this model (c) we obtain an error of ± 0.015 GeV due to uncertainties in the angular $\gamma\gamma^* \to q\bar{q}$ distribution, and ± 0.02 GeV due to uncertainties in the parameters of the Lund model.

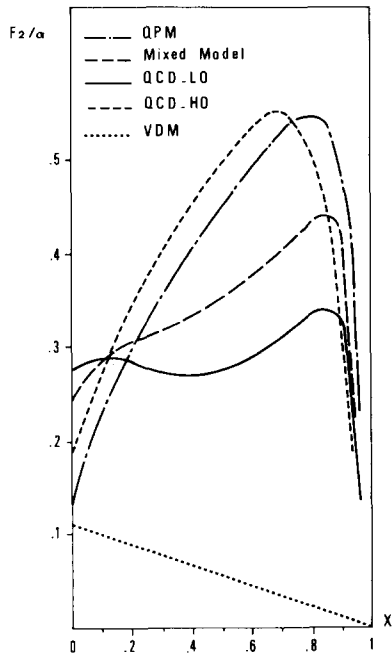Finally, since all models (except for the small soft

Fig. 5. $(1/\alpha)F_2(x)$ curves corresponding to the different fits in the $x > 0.3$ region. Solid curve: QCD LO (u, d, s, c). Dashed curve: QCD LO (u, d, s) plus QPM (c). Dash–dotted curve: QPM (u, d, s, c). Dotted curve: QCD HO (u, d, s, c).

[1] Neglecting the mass of the quasi real photon target (the radiative corrections) would have led to a Λ value about 80 MeV (30 MeV) larger.
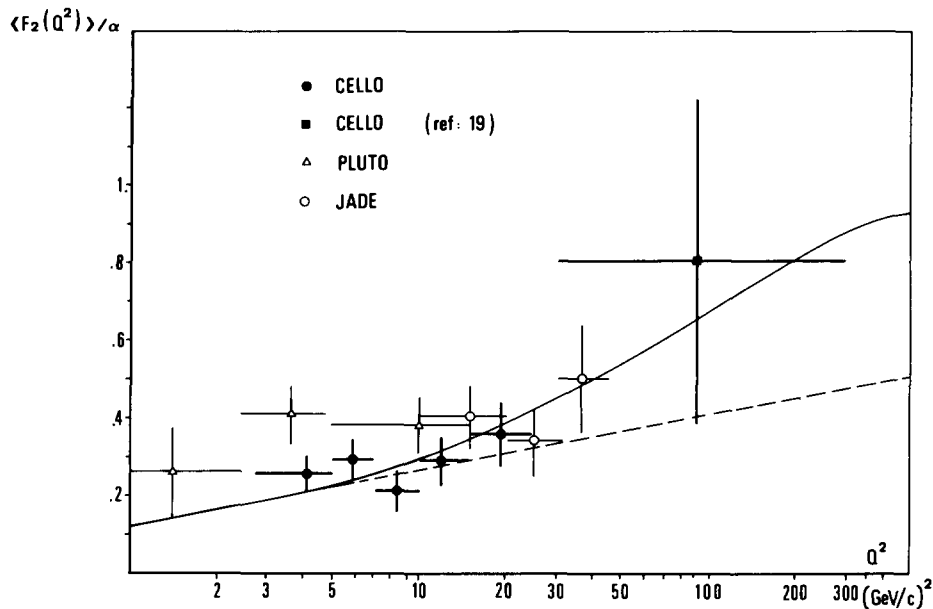
Fig. 6. $(1/\alpha) \langle F_2(x) \rangle$ as a function of Q^2. Solid curve: QCD LO (u, d, s, c) with $\Lambda_{LO} = 0.3$ GeV. Dashed curve = QCD LO (u, d, s).

hadronic piece of the photon due to VDM) predict a Q^2 dependence of the structure function, we have plotted (fig. 6) the mean value of $F_2(x)$ (averaged in the range $0.2 < x < 1.0$) as a function of Q^2. We have included in this figure data from previous experiments [2,3] and also one point coming from our previous work in the high Q^2 range [19]. Clearly data available so far are compatible with a logarithmic variation, without demonstrating the existence of such a dependence.

4. Conclusion

In summary, a measurement of the process $e^+e^- \to e^+e^-$ hadrons has been carried out in the single tag condition. Data are interpreted in terms of deep inelastic scattering of electrons on quasi réal photons. At the average Q^2 of 9 GeV^2/c^2 a good description of the data can be obtained using calculations of the structure functions in the quark parton model and QCD at the leading and next to leading order.

Values of Λ obtained range between 0.07 and 0.28 GeV depending on specific features of the model used. When the light quarks are treated by QCD (LO) and the c quark in the parton model we obtain

$$\Lambda = 0.13^{+0.07}_{-0.05} \text{ (stat)} \pm 0.02 \text{ (syst) GeV} .$$

References

[1] See for example: W.R. Frazer, Fourth Intern. Colloquium on Photon–photon interactions (Paris, 1981); A.J. Buras, Intern. Symp. on Lepton and photon interaction at high energies (Bonn, 1981).
[2] PLUTO Collab., Ch. Berger et al., Phys. Lett. 107B (1981) 168.
[3] JADE Collab., W. Bartel et al., DESY report 82-064 (1982).
[4] CELLO Collab., H.J. Behrend et al., 21st Intern. Conf. on High energy physics (Paris, 1982).
[5] C. Peterson, T. Walsh and P. Zerwas, Nucl. Phys. B174 (1980) 424.
[6] C. Carimalo, J. Parisi and P. Kessler, Phys. Rev. D20 (1979) 1057; D21 (1980) 669.
[7] CELLO Collab., H.J. Behrend et al., Phys. Lett. 126B (1983) 384.

[8] CELLO. A new detector at PETRA, Phys. Scripta 23 (1981) 610.

[9] A.I. Akhiezer and V.B. Berestetskii, Quantum electrodynamics (Interscience, New York, 1965) p. 843.

[10] B. Anderson, G. Gustafson and T. Sjostrand, Z. Phys. C6 (1980) 235;
T. Sjostrand, Lund preprint, LU TP 80-3 (1980);
B. Anderson, G. Gustafson and T. Sjostrand, Nucl. Phys. B197 (1982) 45.

[11] C.T. Hill and G.G. Ross, Nucl. Phys. B148 (1979) 373.

[12] E. Witten, Nucl. Phys. B120 (1977) 189.

[13] C.H. Llewellyn Smith, Phys. Lett. 79B (1978) 83.

[14] W.R. Frazer and J. Gunion, Phys. Rev. D20 (1979) 147.

[15] T. Uematsu and T.F. Walsh, Phys. Lett. B101 (1981) 263.

[16] T. Uematsu and T.F. Walsh, Nucl. Phys. B199 (1982) 93.

[17] W.A. Bardeen and A.J. Buras, Phys. Rev. D20 (1979) 166.

[18] D.W. Duke and J.F. Owens, Phys. Rev. D22 (1980) 2280.

[19] CELLO Collab., H.J. Behrend et al., Phys. Lett. 118B (1982) 211.